applied sciences

MDPI

Article

Comparison of $PM_{2.5}$ in Seoul, Korea Estimated from the Various Ground-Based and Satellite AOD

Sang-Min Kim [1], Ja-Ho Koo [2,*], Hana Lee [2,*], Jungbin Mok [3], Myungje Choi [4,5], Sujung Go [4], Seoyoung Lee [2], Yeseul Cho [2], Jaemin Hong [2], Sora Seo [6], Junhong Lee [7], Je-Woo Hong [8] and Jhoon Kim [2]

1 Environmental Satellite Center, National Institute of Environmental Research, Incheon 22689, Korea; smkim91@korea.kr
2 Department of Atmospheric Sciences, Yonsei University, Seoul 03722, Korea; tjdud9207@yonsei.ac.kr (S.L.); dptmf209@yonsei.ac.kr (Y.C.); rookie820@yonsei.ac.kr (J.H.); jkim2@yonsei.ac.kr (J.K.)
3 Science Systems and Applications, Inc., Lanham, MD 23666, USA; jungbin.mok@nasa.gov
4 Joint Center for Earth Systems Technology, University of Maryland Baltimore County, Baltimore, MD 21250, USA; myungje.choi@nasa.gov (M.C.); sujung.go@nasa.gov (S.G.)
5 NASA Goddard Space Flight Center, Greenbelt, MD 20771, USA
6 Remote Sensing Technology Institute (IMF), German Aerospace Center (DLR) in Oberpfaffenhofen, 82234 Weßling, Germany; sora.seo@dlr.de
7 Max Planck Institute for Meteorology, 20146 Hamburg, Germany; junhong.lee@mpimet.mpg.de
8 Korea Environment Institute, Sejong 30147, Korea; jwhong@kei.re.kr
* Correspondence: zach45@yonsei.ac.kr (J.-H.K.); leehn88@yonsei.ac.kr (H.L.)

Abstract: Based on multiple linear regression (MLR) models, we estimated the $PM_{2.5}$ at Seoul using a number of aerosol optical depth (AOD) values obtained from ground-based and satellite remote sensing observations. To construct the MLR model, we consider various parameters related to the ambient meteorology and air quality. In general, all AOD values resulted in the high quality of $PM_{2.5}$ estimation through the MLR method: mostly correlation coefficients >~0.8. Among various polar-orbit satellite AODs, AOD values from the MODIS measurement contribute to better $PM_{2.5}$ estimation. We also found that the quality of estimated $PM_{2.5}$ shows some seasonal variation; the estimated $PM_{2.5}$ values consistently have the highest correlation with in situ $PM_{2.5}$ in autumn, but are not well established in winter, probably due to the difficulty of AOD retrieval in the winter condition. MLR modeling using spectral AOD values from the ground-based measurements revealed that the accuracy of $PM_{2.5}$ estimation does not depend on the selected wavelength. Although all AOD values used in this study resulted in a reasonable accuracy range of $PM_{2.5}$ estimation, our analyses of the difference in estimated $PM_{2.5}$ reveal the importance of utilizing the proper AOD for the best quality of $PM_{2.5}$ estimation.

Keywords: $PM_{2.5}$; aerosol optical depth (AOD); multiple linear regression; boundary layer height

Citation: Kim, S.-M.; Koo, J.-H.; Lee, H.; Mok, J.; Choi, M.; Go, S.; Lee, S.; Cho, Y.; Hong, J.; Seo, S.; et al. Comparison of $PM_{2.5}$ in Seoul, Korea Estimated from the Various Ground-Based and Satellite AOD. *Appl. Sci.* **2021**, *11*, 10755. https://doi.org/10.3390/app112210755

Academic Editor: Kyung-Hwan Kwak

Received: 31 August 2021
Accepted: 12 November 2021
Published: 15 November 2021

1. Introduction

The negative effects of fine mode particles on human health have been significantly examined, and are more serious at the present time. For example, in addition to the threat to the well-known respiratory and cardiovascular problems, people are currently concerned about the damage to mental health due to the high concentration of aerosols and even precursor gases [1]. This effect has usually been inspected based on the mass density of particulate matter (PM), especially PM having an aerodynamic diameter <2.5 μm ($PM_{2.5}$). To conduct an accurate evaluation, the monitoring of local $PM_{2.5}$ is therefore an essential task. To date, the platform for the in situ measurement of $PM_{2.5}$ has been improved and advanced in many places, resulting in the accumulation of long-term records. Nonetheless, the spatial coverage of in-situ $PM_{2.5}$ observations is still limited, and does not provide abundant data for the evaluation of health effects, particularly in rural regions.

As an alternative approach, satellite remote sensing has been used for the monitoring of aerosol pollution. The aerosol optical depth (AOD) is a product from satellite remote sensing that indicates the atmospheric turbidity associated with the density of airborne particles. However, $PM_{2.5}$ is not directly produced from satellite measurements. Thus, $PM_{2.5}$ estimation using satellite AOD has been widely conducted based on various statistical methods, which are well summarized in [2,3]. Multiple-linear regression (MLR) modeling is a representative method that has been widely used to date, indicating the contribution of various factors (e.g., meteorology) to the estimation of $PM_{2.5}$. Recently, machine learning and deep learning algorithms have been applied to $PM_{2.5}$ estimation, and better results have been achieved compared to the previous approaches.

Nonetheless, the accuracy of $PM_{2.5}$ estimation can vary according to the utilized dataset and methodology. For example, PM estimation can differ between the usage of polar-orbit and geostationary satellite AOD [4], or in accordance with the temporal period [5]. The combination of factors also relates to the quality of the PM estimate [6]. In addition, PM estimation using the same dataset and methodology can result in different levels of quality due only to the difference in spatial location [7].

Although many studies have presented various methods of $PM_{2.5}$ estimation using AOD values, the sensitivity to the type of data used has not been significantly investigated. In particular, the quality of $PM_{2.5}$ estimation according to the kind of AOD, one of the main parameters considered to be significant in the process of $PM_{2.5}$ estimation, has rarely been evaluated. Although some previous works directly compared the spatiotemporal pattern consistency between AOD and $PM_{2.5}$, and diagnosed the difference in terms of the kind of selected AOD values [8,9], evaluation of the quality of estimated $PM_{2.5}$ after advanced statistical data processing was not undertaken.

Thus, this study attempted to examine the impact on the accuracy of $PM_{2.5}$ estimation according to the application of different AOD products, because previous studies showing the effect of different AOD products on the quality of $PM_{2.5}$ estimates are rare. Based on several MLR models, we estimated $PM_{2.5}$ values using multiple AOD values from satellite and ground-based measurements in Seoul. Then, these estimated values were compared with in situ $PM_{2.5}$ observations for validation. Based on the generated statistical parameters, e.g., correlation coefficient (R) and root mean square error (RMSE), we evaluated the $PM_{2.5}$ estimate in terms of sensitivity to the kind of AOD products, seasonal difference, and wavelengths. To identify the seasonal pattern, we used full yearly measurements of AODs from May 2016 to April 2017.

2. Data Description

For the estimation of $PM_{2.5}$ using AODs in this study, we used the multiple remote sensing instruments onboard low-orbit satellites: Moderate Resolution Imaging Spectroradiometer (MODIS) on Terra and Aqua satellites, Visible Infrared Imaging Radiometer Suite (VIIRS) on the Suomi-NPP satellite, Multi-angle Imaging Spectroradiometer (MISR) on the Terra satellite, and Ozone Monitoring Instrument (OMI) on the Aura satellite [10,11]. Each satellite mission has its own retrieval algorithm based on the different wavelength view-angle and spatiotemporal properties. For the MODIS measurement, AOD can be retrieved from both the Dark Target (DT) and Deep Blue (DB) algorithm with a 10×10 km^2 resolution at nadir [12], and the DT AOD retrieval with a 3 km resolution [13]. Here we used these three different AODs, named MODIS-DT, MODIS-DB, and MODIS-3km AODs, respectively. The differences in the specifications of all satellite AODs considered in this study are summarized in Table 1. Although the satellite sensors have multiple channels, AODs in the visible channel around 500–550 nm converted from other channels have been much qualified [11], and are usually considered to be the representative satellite AOD product. Thus, this study only used the satellite AODs at 500 or 550 nm wavelengths. This enabled a better diagnosis of the effect of the retrieval algorithm and spatiotemporal resolution on the $PM_{2.5}$ estimation.

Table 1. Detail description of satellite AOD values used in this study.

Data Name	Description				
	Satellite	Wavelength (nm)	Spatial Resolution (km^2)	Retrieval Algorithm	Observation Time (UTC)
MODIS-DT	Terra Aqua	550	10 × 10	C6	01:20–03:25 03:35–05:40
MODIS-DB	Terra Aqua	550	10 × 10	C6	01:20–03:25 03:35–05:40
MODIS-3km	Terra Aqua	550	3 × 3	C6	01:20–03:25 03:35–05:40
VIIRS	Suomi-NPP	550	6 × 6	EDR	03:15–05:40
MISR	Terra	550	17.6 × 17.6	V22	01:30
OMI	Aura	500	13 × 24	Near-UV	04:05–05:35

In addition to the satellite AOD measurements, we also utilized AODs from multiple ground-based measurements. Due to the participation of the KOREA-US air quality (KORUS-AQ) campaign [14], several ground-based remote sensing instruments were installed concurrently in May 2016 at the top of the Science Hall in Yonsei University, South Korea (37.564° N, 126.935° E), and maintained observations until April 2017: a sun-photometer registered in the Aerosol Robotic Network (AERONET), a skyradiometer registered in the SKYNET, a Brewer spectrophotometer, and two Multi-Filter Rotating Shadowband Radiometers (MFRSR), as summarized in Table 2 [15–20]. Because these are remote sensing instruments, AOD measurement is only available in daytime, from sunrise to sunset. AERONET and SKYNET AODs are generally produced each 20 min, the MFRSR AOD is per 5 min, and AOD of the Brewer spectrophotometer is per 1 h. To ensure consistency, we used the daily mean AOD for all instruments. In contrast to the satellite AOD, we used ground-based AOD observations at multiple channels (wavelengths) because this approach has been more intensively validated [21–23]. Because the ground-based instruments better reflect the local air properties and have better accuracy than the satellite measurements, the usage of these ground-based AOD observations enable inspection of the performance of $PM_{2.5}$ estimation according to the channel of the AODs.

Table 2. Detailed description of ground-based AOD data used in this study.

Data Name	Instrument	Wavelength (nm)	Retrieval Algorithm
AERONET	CIMEL Electronique CE318 multiband sun photometer	340, 380, 440, 500, 675, 870, 1020, 1640	[15]
SKYNET	POM-02 Skyradiometer	340, 380, 400, 500, 675, 870, 1020	[16,17]
UV-MFRSR VIS-MFRSR	Multi-Filter Rotating Shadowband Radiometers (MFRSR)	305, 311, 325, 332, 340, 380 (UV-MFRSR) 415, 440, 500, 615, 673, 870 (VIS-MFRSR)	[18,19]
Brewer spectrophotometer	Brewer Spectrophotometer (MK-IV, No. 148)	320	[20]

In order to prepare an effective MLR model for the PM estimation using various AODs, as described in the next section, a number of meteorological and physical variables are necessary. Planetary boundary layer height (PBLH) is one of the essential pieces of information in the conversion process between column-integrated and surface-level data [24]. In this study, we used the PBLH data retrieved from the ceilometer measurement at the top of the Science Hall in Yonsei University. The process of PBLH calculation was well described in [25]. For comparison purposes, we also used the PBLH from the European Centre for Medium-Range Weather Forecasts (ECMWF) reanalysis data, ERA-Interim. Additionally, we used several meteorological parameters, such as air temperature, relative humidity, wind speed, and visibility. These meteorological parameters in the Korean peninsula are routinely monitored at the Automatic Weather Station (AWS) operated by the Korea Meteorological Administration (KMA). For this study, we used meteorological data

of the Songwol-dong AWS station, which is the closest site (~2 km) to Yonsei University. We also used the amounts of $PM_{2.5}$, surface ozone, and nitrogen dioxide (NO_2) measured at the Seodaemun-gu surface station, which is the closest air pollution monitoring site to Yonsei University (~1.5 km). Both ozone and NO_2 data were obtained from the AIRKOREA data archive (https://www.airkorea.or.kr/, final accessed on 1 January 2021) and the unit is parts per billion (ppb). The quality control and assurance process was confirmed by the AIRKOREA data archive system; therefore, the minimum quality of $PM_{2.5}$, ozone, and NO_2 was ensured guaranteed. The analysis in this study was only performed when the $PM_{2.5}$ values were available. The site information of Yonsei University was described in detail in Jung et al. (2010) [26].

3. Methodology

Although AOD from space-borne satellite measurement provides a quantitative pattern of aerosol loadings in the Earth's atmosphere, AOD cannot be converted directly into a $PM_{2.5}$ value because AOD is a columnar amount and indicator of atmospheric turbidity; this is different from the physical meaning of $PM_{2.5}$, which is a surface mass density. Thus, a specific process is required to convert the columnar AOD to the surface $PM_{2.5}$. MLR modeling has been widely utilized for this purpose. Although the application of machine learning or deep learning techniques have recently started to produce meaningful results for the conversion between AOD and $PM_{2.5}$ [4–7], the MLR method continues to be frequently used for PM estimation using AOD values due to its simplicity and convenience in assessing the influence of considering factors [27,28]. In addition, the performance of the MLR method for PM estimation is comparable with that of other advanced techniques [29]. Therefore, to evaluate how different AOD values influence the PM estimation, we used the MLR method in this study.

A number of factors are considered in the MLR model for $PM_{2.5}$ estimation from AOD values. PBLH plays an important role in determining the effective height of homogeneous mixing of local particles near the surface, and assisting in the detection of the contribution of lower layer air pollution to the total column of aerosol amount. Wind speed indicates the effect of the degree of dispersion on the accumulation or ventilation of airborne aerosols [4,30]. Relative humidity relates to the growth in the particle size and mass [24], and air temperature can be associated with the source of long-range transport [31] or the extent of precursor emissions from biogenic sources [32]. Visibility is another well-known indicator of aerosol pollutions [33]. Ozone and NO_2 can show the local photochemical activity [34] and atmospheric chemical conditions related to the aerosol pollutions [35,36].

Based on these data, we constructed MLR models having different combinations of variables. The description and variables used for each MLR model are shown in Table 3. MLR Model 1 (M1) is the simplest model, and estimates $PM_{2.5}$ only based on the direct linear regression with AOD, which is still significantly investigated for the diagnosis of PM exposure [37]. MLR Model 2 (M2) estimates $PM_{2.5}$ using PBLH in addition to AOD, considering the effective height of aerosol accumulation near the surface. MLR Model 3 (M3) includes not only meteorological factors (temperature, wind speed, relative humidity, and visibility) but also chemical conditions in the atmosphere (ozone and NO_2). For M2 and M3, we utilized two different PBLH data, which were obtained from ceilometer observation (related to M2-1 and M3-1) and from ECMWF reanalysis (related to M2-2 and M3-2).

MLR models were established using 50% of all available data selected randomly, and evaluated with the remaining 50% of the data. Figure 1 shows the validation example of all MLR models (M1, M2-1, M2-2, M3-1, and M3-2) using AODs retrieved from the MODIS-DT algorithm. Considering the reverse pattern of AOD and $PM_{2.5}$ in East Asia [38], the relationship between observed and estimated $PM_{2.5}$ from the M1 model (i.e., only AOD is considered) is acceptable, having a linear shape and moderate correlation coefficient (R). However, the slope was 0.15, indicating that the estimated $PM_{2.5}$ cannot follow the variation range of observed $PM_{2.5}$. When we included the PBLH parameter in the MLR

model (M2), the correlation improved and the slope increased slightly. However, the quality enhancement of M2 model does not look to be significant.

Table 3. Detailed description of statistical models applied in this study for the $PM_{2.5}$ estimation using AOD data (PBLH: planetary boundary layer height, RH: relative humidity, and B: intercept value. F(RH) is equal to 1/{1 – (RH / 100)}, referring to Seo et al. (2015) [24]. The units of the data used are as follows: $PM_{2.5}$ (μg/m^3), AOD (unitless), PBLH (km), temperature (K), wind speed (m/s), visibility (km), RH (%), NO_2 (ppb), O_3 (ppb).

Models	Description
M1	$PM_{2.5}$ = AOD + B
M2-1	$PM_{2.5}$ = AOD/PBLH (ceilometer) + B
M2-2	$PM_{2.5}$ = AOD/PBLH (ECMWF reanalysis) + B
M3-1	$PM_{2.5}$ = AOD + PBLH (ceilometer) + Temperature + Wind speed + Visibility + f (RH) + NO_2 + O_3 + B
M3-2	$PM_{2.5}$ = AOD + PBLH (ECMWF reanalysis) + Temperature + Wind speed + Visibility + f (RH) + NO_2 + O_3 + B

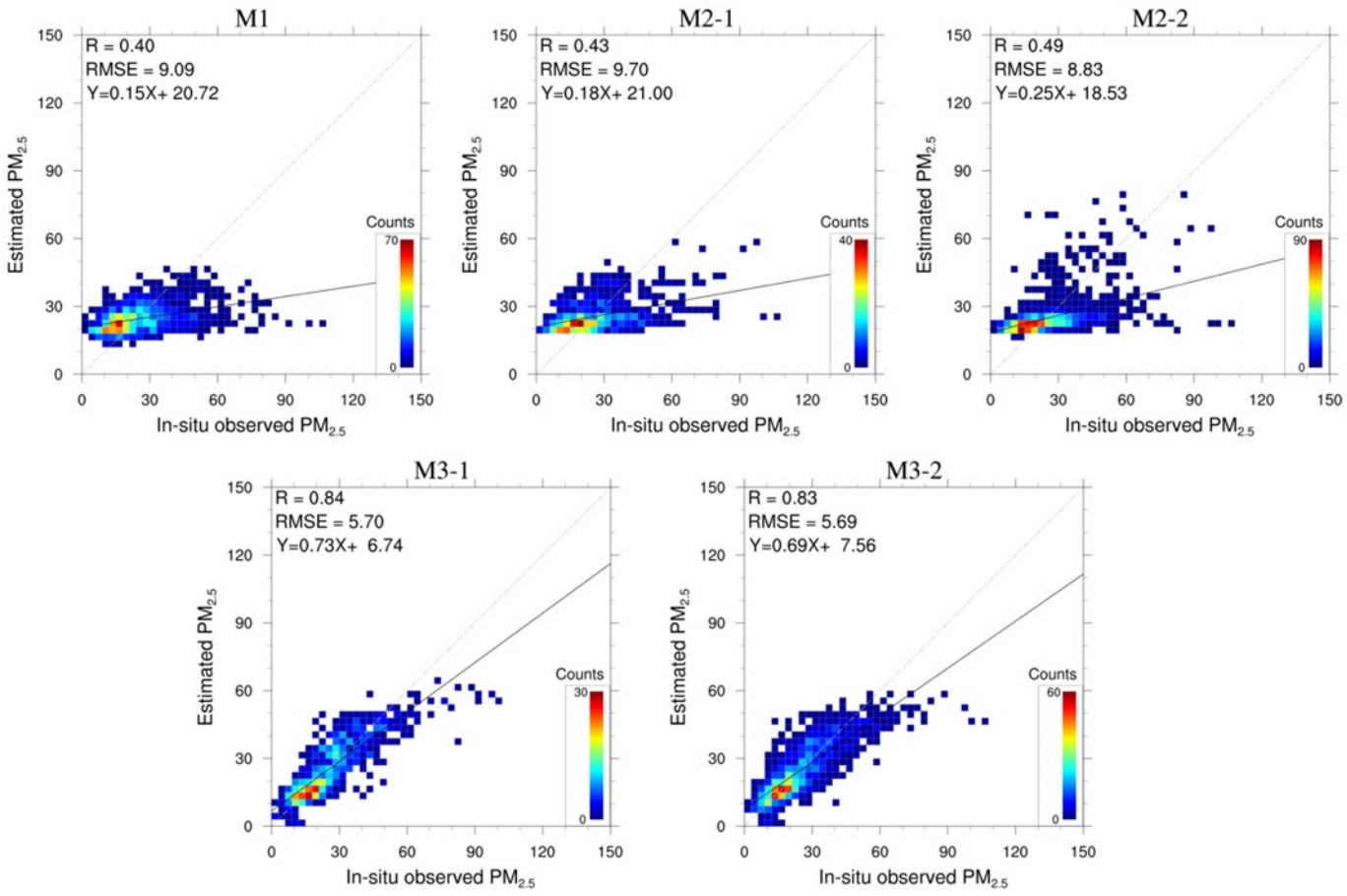

Figure 1. Comparison between in situ observed and estimated $PM_{2.5}$ (unit: μg/m^3) using MODIS-DT AOD values based on 5 statistical models in this study (M1, M2-1, M2-2, M3-1, and M3-2). Colors indicate the occurrence of each case. The dashed line is the 1:1 line and the solid line shows the linear regression pattern.

After including the mentioned meteorological and chemical factors (M3), the performance of the MLR model was finally significantly enhanced: R > 0.8 between observed and estimated $PM_{2.5}$ and the slope was ~0.7. Although the M3 model still underestimated the observed $PM_{2.5}$, especially in heavily polluted conditions ($PM_{2.5}$ > 60 μg/m^3), these results indicate that the MLR model considering AOD, PBLH, and some meteorological and

chemical conditions results in a reliable quality in $PM_{2.5}$ estimation, that was comparable to the machine-learning approaches [29]. An additional comparison was made to assess the effect of using different PBLH data. We did not find large differences in the results between M2-1 and M2-2, or between M3-1 and M3-2, implying that the data source of PBLH does not have a significant influence. Overall, this demonstrates the usefulness of MLR modeling for the $PM_{2.5}$ estimation. Based on this finding, deeper analyses of the MLR model results are continued in Section 4.

4. Results and Discussions

First, compared the $PM_{2.5}$ estimation of all MLR models using different satellite AOD data (Table 4). For the M1 and M2 models, the performance of $PM_{2.5}$ estimation seems largely dependent on the used AOD; the cases of MODIS and MISR AOD show higher correlation and lower RMSE, but those of VIIRS and OMI AOD show lower correlation and higher RMSE. However, the M3 model results reveal the consistency of $PM_{2.5}$ estimation for all AOD cases. All correlation coefficients are higher 0.7 and their difference is smaller than 0.2; these values are significantly better than the cases of the M1 and M2 models, which show correlations < 0.5 and correlation differences > 0.3. In terms of slope, M1 and M2 show relatively small slopes: all slopes of M1 and M2 < 0.3. However, M3 results show a significantly better slope, which is from 0.5 to 0.7. Comparison between M3-1 and M3-2 indicates that M3-1 can estimate $PM_{2.5}$ slightly better, implying that the ground-based measurement of PBLH can better represent the local conditions of aerosol distribution.

Table 4. R, RMSE, slope, and used data number (N) of correlations between measured and estimated $PM_{2.5}$ (unit: $\mu g/m^3$) values for five MLR models (M1, M2, M2-1, M3-1, and M3-2) using six satellite AODs. The unit of RMSE is $\mu g/m^3$.

Statistics	MLR Model	MODIS-DT	MODIS-DB	MODIS-3km	VIIRS	MISR	OMI
R	M1	0.4	0.48	0.36	0.29	0.36	0.17
	M2-1	0.43	0.54	0.43	0.21	0.45	0.24
	M2-2	0.49	0.46	0.46	0.26	0.49	0.21
	M3-1	0.84	0.83	0.84	0.8	0.85	0.75
	M3-2	0.83	0.81	0.81	0.8	0.83	0.75
RMSE	M1	9.09	9.53	9.11	9.5	11.4	10.75
	M2-1	9.7	8.9	9.61	9.85	12.83	10.78
	M2-2	8.83	9.74	8.77	9.59	10.65	10.69
	M3-1	5.7	5.9	5.76	5.99	7.45	7.36
	M3-2	5.69	6.25	5.72	6.09	7.33	7.32
Slope	M1	0.15	0.22	0.14	0.08	0.13	0.01
	M2-1	0.18	0.28	0.19	0.05	0.23	0.03
	M2-2	0.25	0.21	0.2	0.08	0.23	0.02
	M3-1	0.73	0.71	0.69	0.63	0.72	0.55
	M3-2	0.69	0.67	0.68	0.62	0.69	0.57
N	M1	1643	2794	1933	3027	249	577
	M2-1	877	1662	1049	1608	146	318
	M2-2	1639	2786	1930	3027	249	577
	M3-1	843	1597	1012	1608	146	318
	M3-2	1576	2686	1863	2900	243	557

Overall, MODIS-DT AOD results in the best quality of $PM_{2.5}$ estimation: the highest correlation coefficient, smallest RMSE, and largest slope. Other MODIS AODs (MODIS-DB and MODIS-3km) show a similar performance. MISR AOD shows a high correlation and large slope, but RMSE is high, probably due to the small data number (Table 4). VIIRS AOD does not result in high accuracy of $PM_{2.5}$ estimation in the M1 and M2 models; in particular, the slope is relatively small (<0.1), indicating a weak sensitivity of the estimated $PM_{2.5}$ to the observed value. However, VIIRS AOD results in highly enhanced accuracy of $PM_{2.5}$ estimation in the M3 model. The reason for this drastic enhancement is not clear,

but perhaps can be explained by the larger number of data than that of other AODs. In turn, this is attributable to a larger swath width because statistical modeling is generally more advantageous with a larger dataset. OMI AOD results in relatively lower quality of $PM_{2.5}$ estimation, but the M3 result is acceptable, showing a moderate correlation coefficient (R = ~0.7). The low spatial resolution of OMI L1B data (13 × 24 km^2), and generally unfavorable conditions of cloud masking in aerosol retrieval, may result in a lower correlation coefficient. Here, we confirm that the choice of AOD to be applied can influence the performance of $PM_{2.5}$ estimation, but that any AOD can contribute to the moderate quality of $PM_{2.5}$ estimation when the MLR model is composed of PBLH with other meteorological and chemical information.

Based on the result of the M3-1 model, which recorded the best performance, the seasonal pattern of estimated $PM_{2.5}$ was also analyzed (Figure 2). Compared to the observed $PM_{2.5}$, the estimated $PM_{2.5}$ shows the highest correlation (R = ~0.8 to 0.9) and slope (~0.7 to 0.9) in autumn (September–October–November, SON), implying that the columnar AOD has a relatively high sensitivity to the variation in surface fine-mode particles during this season. Given that there are a number of springtime Asian dust events and summertime hygroscopic growth of local aerosols in the Korean peninsula [39,40], AOD in spring and summer can be partially affected by coarse-mode particles, resulting in relatively lower correlations and slope values. The RMSE pattern looks similar, i.e., small RMSE in autumn (i.e., higher quality) but large RMSE in spring (i.e., lower quality). RMSE in summer is relatively small because $PM_{2.5}$ is the lowest in summer.

The performance of $PM_{2.5}$ estimation in spring, summer, and autumn does not show a significant discrepancy according to the AOD used. In winter, however, the quality of $PM_{2.5}$ estimation is relatively dependent on the AOD used. Although the MISR AOD results in the highest correlation (R = ~0.9) and slope (~0.9), the OMI AOD results in the lowest correlation (R = ~0.65) and slope (<~0.5), and highest RMSE, indicating a weak capability of capturing the surface aerosol properties in winter. MODIS AODs also show different performances: MODIS-3km and MODIS-DT AOD are related to a high correlation and slope, but MODIS-DB is related to a relatively low correlation and slope.

This feature indicates that the consistency of various satellite AOD data is not high in winter. It appears that the number of data is not significantly associated with the quality of $PM_{2.5}$ estimation (Figure 2a). This inconsistency may be attributed to the accuracy of AOD retrieval in winter. The quality of AOD retrieval can be degraded due to a high solar zenith angle [41,42] or bright surface albedo caused by snow cover [43,44], which are representative of winter conditions on the Korean peninsula. Some retrieval algorithms can be largely affected by the winter characteristics of surface albedo. For example, the MODIS DT algorithm selects the minimum surface albedo in 30-day data for each pixel, and the high-reflecting surface case can be selected if there retains a snow-covered surface for a long period during winter. Different particle shapes can be associated with the variation in AOD quality if combined with the other influencing factors noted above (e.g., SZA and surface albedo). Aerosol retrieval of MISR using multi-view angles appears to be more advantageous for the separation of surface and aerosol signals than other sensors, resulting in better reliability in retrieved AOD across seasons. Therefore, according to the specification of satellite sensors and properties of the retrieval algorithm, the AOD difference can be relatively larger in winter. Further research will be required to reduce the gap in the $PM_{2.5}$ estimation in winter. Because aerosol pollution in South Korea is most serious during winter [45], the quality improvement in wintertime $PM_{2.5}$ estimation is essential.

Because we found that the MODIS AOD values resulted in different performance of $PM_{2.5}$ estimation according to the retrieval algorithm, we also inspected if the result of $PM_{2.5}$ estimation was different when the MODIS AOD of the Terra (or Aqua) satellite is only used. Figure 3 shows the comparison of correlation, slope, and RMSE results between observed and estimated $PM_{2.5}$ when the MODIS-DT, MODIS-DB, and MODIS-3km onboard the Terra (or Aqua) satellite AOD was used with M3-1 and M3-2 models. It

does not appear that an obvious change was derived from this comparison but, in general, the MODIS AODs onboard the Terra satellite resulted in a slightly higher accuracy. The difference in the correlation coefficients appears negligible, but the slope difference between the Terra and Aqua AOD cases is sometimes significant (higher that 0.05 difference). The number of data of the MODIS AODs of the Terra satellite are slightly higher but this does not appear to be a critical factor. One significant difference is the temporal difference; the overpassing time of the Terra satellite is around 10:30 AM local time, whereas that of Aqua satellite is around 1:30 PM local time. Considering that PBLH is generally higher in the afternoon compared to the morning due to the enhanced vertical mixing driven by the surface heating [21,46], it is feasible to expect a smaller portion of surface aerosol concentration in the total columnar aerosol density, which may explain the relatively lower accuracy of the estimated $PM_{2.5}$. This comparison provides an insight into identifying the role of AOD measurement time in $PM_{2.5}$ estimation.

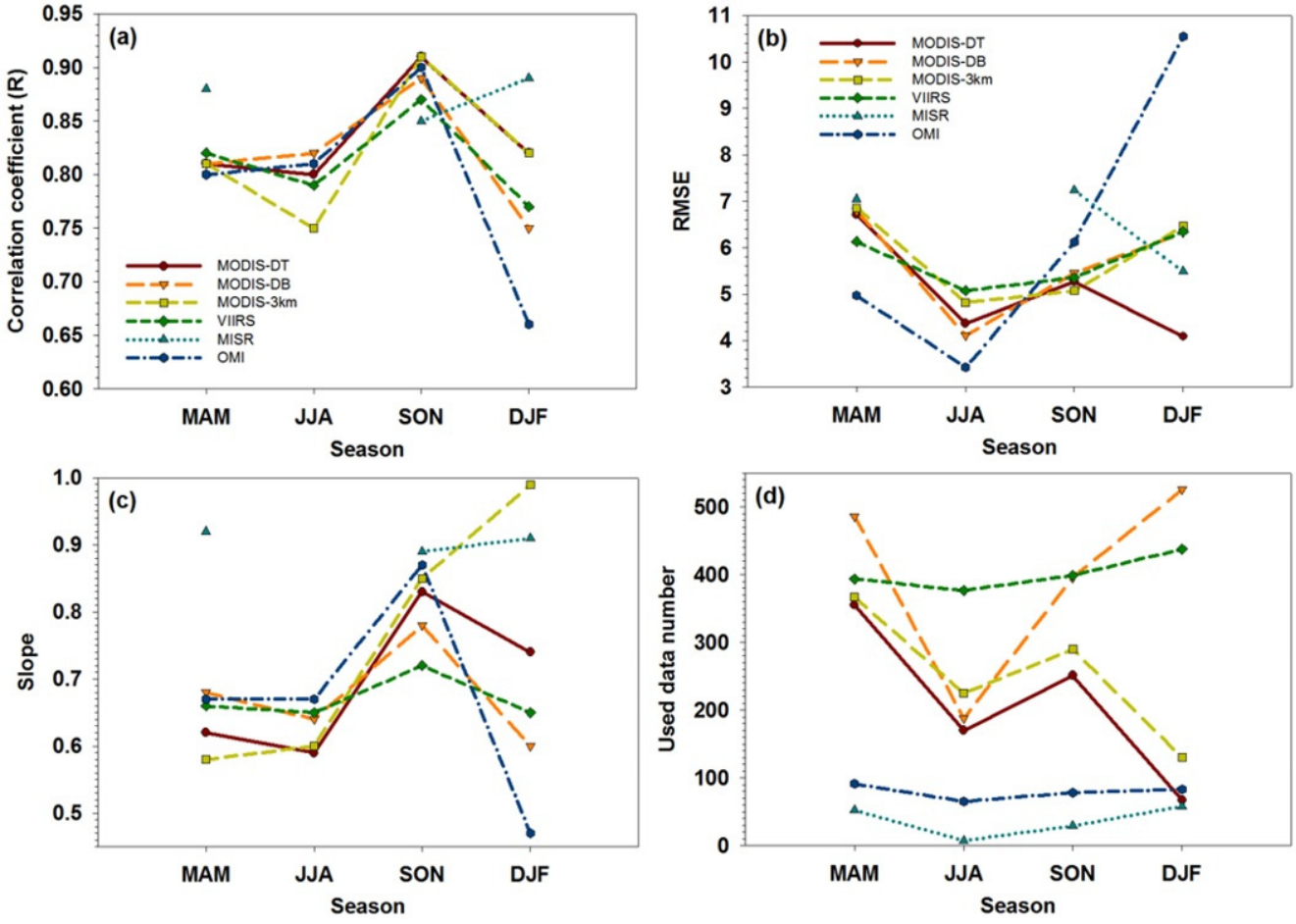

Figure 2. Seasonal variation in (**a**) R, (**b**) RMSE, (**c**) slope, and (**d**) number of data used in correlations between measured and estimated $PM_{2.5}$ (unit: $\mu g/m^3$) values. Estimated $PM_{2.5}$ values here are from the M3-1 model using MODIS-DT (red), MODIS-DB (orange), MODIS-DT for 3 × 3 km resolution (yellow green), VIIRS (green), MISR (light blue), and OMI (blue) AOD. MAM means March–April–May (spring), JJA means June–July–August (summer), SON means September–October–November (autumn), and DJF means December–January–February (winter). The unit of RMSE is $\mu g/m^3$.

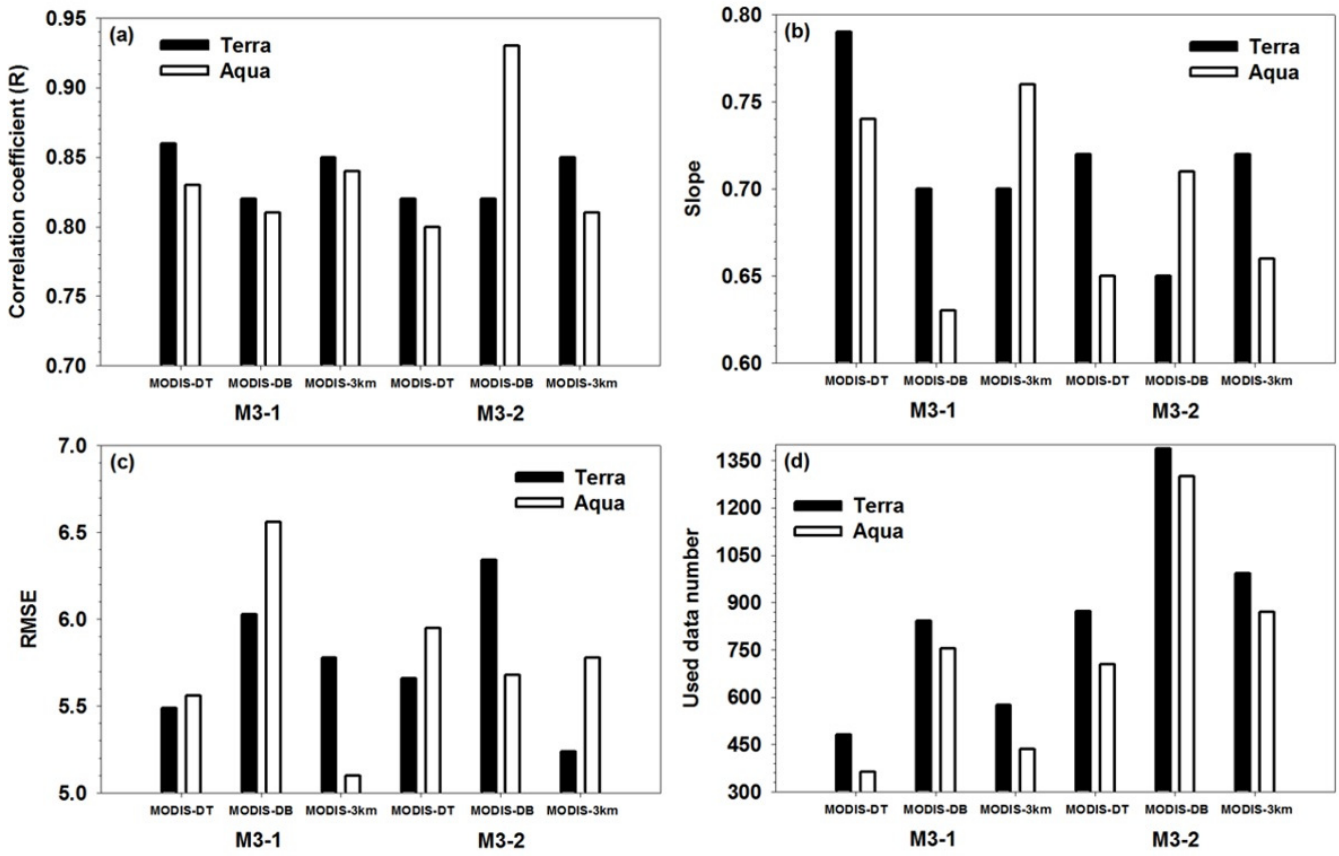

Figure 3. Provision of (**a**) R, (**b**) slope, (**c**) RMSE, and (**d**) number of data used for the comparison between measured and estimated $PM_{2.5}$ from M3-1 and M3-2 models with the usage of MODIS-DT, MODIS-DB, and MODIS-3km AODs. Black bars indicate results from AODs of the Terra satellite, and white bars indicate results from AODs of the Aqua satellite. The unit of RMSE is $\mu g/m^3$.

Thus far, we examined the relationship between the performance of $PM_{2.5}$ estimation and applied satellite AOD values. Next, similar comparisons were repeated using the various ground-based AODs. As mentioned, we estimated $PM_{2.5}$ based on the M3-1 model using AERONET, SKYNET, ultraviolet MFRSR (UV-MFRSR), visible MFRSR (VIS-MFRSR), and Brewer spectrophotometer AOD (Figure 4). Here, one more key point was to investigate the performance of $PM_{2.5}$ estimation in terms of the channel (wavelength) of AOD. We mainly compared the basic MLR (M1) and the best MLR (M3-1) model results. M1 results, only considering AOD for $PM_{2.5}$ estimation, show a large wavelength dependence: a decrease in the correlation coefficients and slope, and an increase in RMSE for the comparison between observed and estimated $PM_{2.5}$ as the wavelength increased. AODs in near-infrared (IR) channels do not result in high-quality $PM_{2.5}$ estimation. This feature reveals the importance of channel selection in the simple application of the relationship between AOD and $PM_{2.5}$ for the investigation of regional aerosol pollution. Considering the large wavelength dependence of ground-based AOD measurement [47], exact examination of the relationship between AOD and $PM_{2.5}$ cannot be guaranteed without the appropriate channel selection. This lesson should be significantly considered for the usage of AOD to connect with the level of $PM_{2.5}$ directly [37].

When the M3 model is used, however, the wavelength dependence does not occur (Figure 4d–f). From this result, we find that the wavelength dependence of AOD is not influential on the $PM_{2.5}$ estimation if the advanced statistical approach is applied with a number of other effective factors (i.e., PBLH, meteorology, local chemical concentration). The M3 results reveal that both MFRSR AOD values result in a high accuracy of $PM_{2.5}$ estimation because MFRSR AODs here are retrieved with the elaborate screening of Rayleigh scattering induced by trace gases such as ozone and NO_2 [23], resulting in the more precise

capture of local aerosol variation. Compared to the results obtained from using the satellite AODs (Table 4), the usage of ground-based AODs shows similar correlation coefficients but a slightly higher RMSE and lower slope. This feature can probably be explained by the fact that ground-based AODs more reflect the local characteristic of the maximum aerosol pollution because the statistical approach has limitations in the detection of dense aerosol pollution [4].

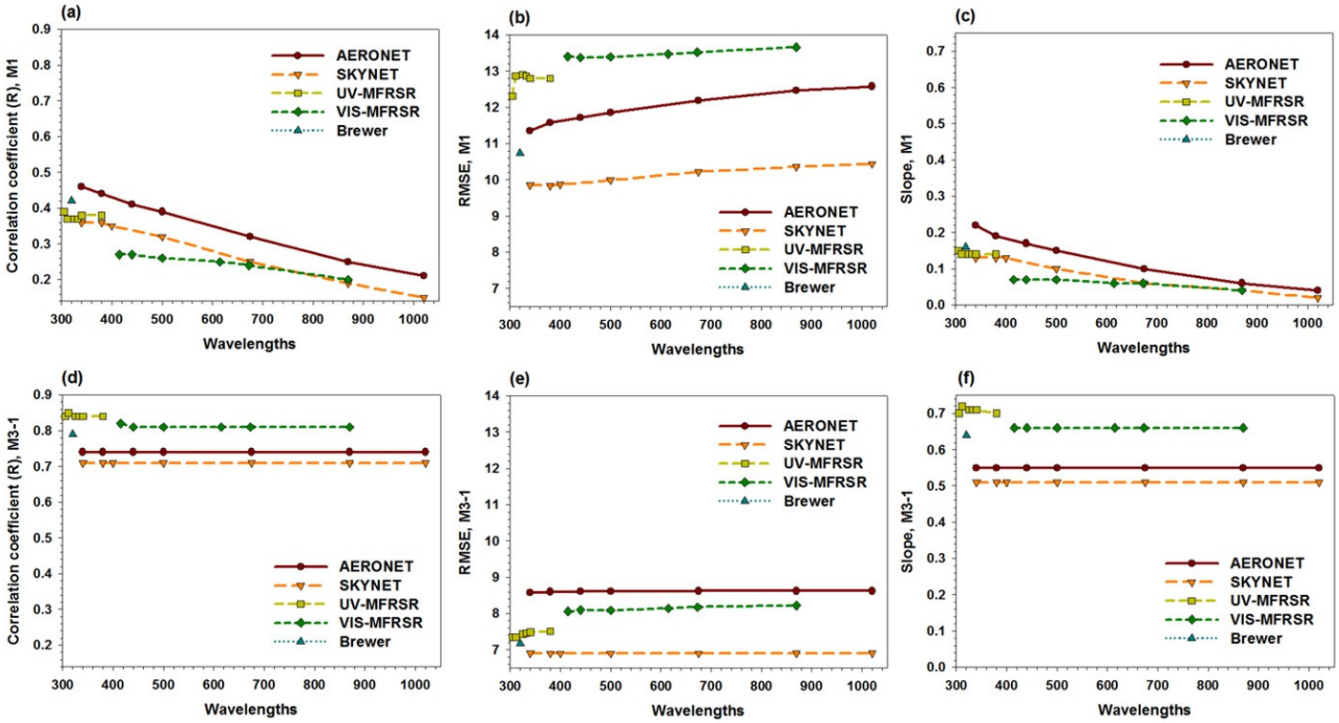

Figure 4. Wavelength dependence of (**a**) R, (**b**) RMSE, and (**c**) slope values of the M1 model, and that of (**d**) R, (**e**) RMSE, and (**f**) slope values of the M3-1 model using multiple ground-based AODs. The unit of RMSE is $\mu g/m^3$.

The interesting result shown in Figure 4—the performance of $PM_{2.5}$ estimation using the UV- and VIS-MFRSR AODs— is described here in more detail. The M1 results show that the quality of estimated $PM_{2.5}$ based on MFRSR AODs is lower than that of the others. In contrast, the quality of estimated $PM_{2.5}$ based on MFRSR AODs appears to be the best when the M3 model is applied, obtaining the highest correlations and slope values. The main difference of UV- and VIS-MFRSR AODs from other AODs is the consideration of the ozone and NO_2 optical depth. Namely, the variation in Rayleigh scattering by ozone and NO_2 is accurately considered in the retrieval of UV- and VIS-MFRSR AOD following the methodology in Mok et al. (2018) [19], whereas the climatology of ozone and NO_2 is only considered in the retrieval of AERONET and SKYNET AODs. It appears that the AOD performance itself is better for the AERONET and SKYNET AODs, probably due to the better detection of direct sun (the AERONET and SKYNET instruments follow the diurnal cycle of the solar position), resulting in more accurate $PM_{2.5}$ estimation using the M1 model. However, in the M3 model where the variation of meteorological and chemical (ozone and NO_2) factors is considered, accurate consideration of ozone and NO_2 optical depth in UV- and VIS-MFRSR AOD appears to be more influential on the estimation of qualified $PM_{2.5}$. The study site, Yonsei University, is located near a road where high traffic generally occurs [26]. We note that the usage of local air pollutants in the MLR model also appears to be significant for the $PM_{2.5}$ estimation, particularly for the polluted region.

Finally, we examined the seasonal variation in $PM_{2.5}$ estimation using ground-based AODs in multiple channels. Table 5 shows a comparison of correlation coefficients, RMSE, and slope between the observed $PM_{2.5}$ and $PM_{2.5}$ estimated from the usage of AERONET AODs in the M3-1 model, as a representative example, during each season. Similar to

the usage of satellite AODs (Table 4), the performance of $PM_{2.5}$ estimation is the best in autumn, which obtained the highest correlation coefficient, lowest RMSE, and highest slope. Although the quality of $PM_{2.5}$ estimation appears to be relatively lower in spring, probably due to the large reflection of Asian dust events near the surface, $PM_{2.5}$ estimation appears to be reliable for all seasons, even winter. This difference between the usage of satellite and ground-based AODs implies that the inconsistency of $PM_{2.5}$ estimation in winter may be attributed to the surface conditions, because the AOD retrieval from the ground-based measurement is not significantly associated with the surface reflectance. In addition, no wavelength dependence of AOD was found for each season, meaning that the channel selection of AOD is not of concern if the statistical approaches are applied for $PM_{2.5}$ estimation.

Table 5. Seasonal variation of R, RMSE, slope, and number of data used (N) in correlations between measured and estimated $PM_{2.5}$ (unit: $\mu g/m^3$) values for various wavelengths. Estimated $PM_{2.5}$ values here are from the M3-1 model using AERONET AOD. The unit of RMSE is $\mu g/m^3$.

AERONET AOD		M3-1						
		340 nm	380 nm	440 nm	500 nm	675 nm	870 nm	1020 nm
Spring	R	0.74	0.74	0.74	0.73	0.73	0.73	0.73
	N	951	953	953	953	953	953	953
	RMSE	9.83	9.86	9.89	9.91	9.95	9.97	9.98
	Slope	0.54	0.54	0.53	0.53	0.53	0.53	0.53
Summer	R	0.79	0.78	0.78	0.78	0.78	0.78	0.78
	N	337	343	343	343	343	343	343
	RMSE	6.99	6.82	6.83	6.84	6.86	6.86	6.87
	Slope	0.62	0.66	0.66	0.66	0.66	0.66	0.66
Autumn	R	0.81	0.82	0.82	0.82	0.82	0.82	0.82
	N	511	513	513	513	513	513	513
	RMSE	5.58	5.50	5.51	5.51	5.54	5.56	5.57
	Slope	0.68	0.67	0.67	0.67	0.66	0.66	0.66
Winter	R	0.78	0.76	0.76	0.76	0.76	0.76	0.76
	N	770	774	774	774	774	774	774
	RMSE	6.98	7.03	7.04	7.04	7.04	7.04	7.04
	Slope	0.61	0.61	0.61	0.61	0.61	0.61	0.61

5. Summary and Conclusions

Based on the MLR method, this study evaluated the accuracy of $PM_{2.5}$ estimation in accordance with the type of applied AOD value. We confirmed that all satellite AODs generally resulted in satisfactory $PM_{2.5}$ estimation if other influential factors (e.g., PBLH, local meteorology, and the quantity of precursor gases) were simultaneously considered. In spite of this positive result, we also obtained some inconsistent results in winter, when the AOD retrieval can have larger uncertainty. Because the aerosol pollution in the Korean peninsula is usually the most serious in winter, an effort to identify the proper AOD appears to be required to achieve high accuracy of $PM_{2.5}$ estimation. The overpassing time of satellite measurements may have an impact on $PM_{2.5}$ estimation, but may not be significant. The direct relationship between AOD and $PM_{2.5}$ shows a relatively large wavelength dependence, which is negligible, however, if the MLR method is applied. In conclusion, the type of AOD does not significantly affect the accuracy of PM estimation but, nonetheless, careful usage appears to be required if a specific condition is the research target (e.g., diurnal or seasonal variation).

Numerous studies have been previously conducted about the estimation of PM using AOD values based on many different statistical methods. Through these works, we determined which factors are significant and should be considered to ensure the quality of $PM_{2.5}$ estimation, and recognized the substantial effect of the AOD contribution. Because a number of different AOD values are produced by various satellite and ground-based measurements, it is necessary to determine how the performance of $PM_{2.5}$ estimation

can change in terms of applied AOD values. Our research provides useful information about this phenomenon and improvements in the search for an approach for better $PM_{2.5}$ estimation from AOD values.

Author Contributions: Conceptualization, S.-M.K. and J.-H.K.; methodology, S.-M.K., J.-H.K., M.C., S.S. and J.K.; software, S.-M.K. and S.S.; validation, S.-M.K., J.-H.K., M.C. and J.H.; formal analysis, S.-M.K. and J.-H.K.; investigation, S.-M.K., J.-H.K. and J.H.; resources, H.L., J.M., M.C., S.G., S.L., Y.C., J.L. and J.-W.H.; data curation, H.L., J.M., M.C., S.G., S.L., Y.C., J.L. and J.-W.H.; writing—original draft preparation, S.-M.K. and J.-H.K.; writing—review and editing, J.-H.K. and H.L.; visualization, S.-M.K., H.L. and J.H.; supervision, J.-H.K., H.L. and J.K.; project administration, J.-H.K. and J.K.; funding acquisition, S.-M.K., J.-H.K. and J.K. All authors have read and agreed to the published version of the manuscript.

Funding: This work was supported by Institute for Information & communications Technology Promotion (IITP) grant funded by the Korea government (MSIP) (2021-0-00459, Development of a Service Platform for Improving the Accuracy of Particulate Matter Forecast). This work was also supported by a grant from the National Institute of Environmental Research (NIER), funded by the Ministry of Environment (MOE) of the Republic of Korea (NIER-2021-01-01-100).

Institutional Review Board Statement: Not applicable.

Informed Consent Statement: Not applicable.

Data Availability Statement: The AERONET data are available from https://aeronet.gsfc.nasa.gov. The MODIS Dark Target, Deep Blue, OMI, and MISR aerosol data are available from https://earthdata.nasa.gov/. The VIIRS aerosol data are available from class.noaa.gov. All data were accessed finally on 31 January 2021.

Acknowledgments: This work was supported by Institute for Information & communications Technology Promotion (IITP) grant funded by the Korea government (MSIP) (2021-0-00459, Development of a Service Platform for Improving the Accuracy of Particulate Matter Forecast). This work was also sup-ported by a grant from the National Institute of Environmental Research (NIER), funded by the Ministry of Environment (MOE) of the Republic of Korea (NIER-2021-01-01-100).

Conflicts of Interest: The authors declare no conflict of interest. The funders had no role in the design of the study; in the collection, analyses, or interpretation of data; in the writing of the manuscript, or in the decision to publish the results.

References

1. Shin, J.; Park, J.Y.; Choi, J. Long-term exposure to ambient air pollutants and mental health status: A nationwide population-based cross-sectional study. *PLoS ONE* **2018**, *13*, e0195607. [CrossRef] [PubMed]
2. Chu, Y.; Liu, Y.; Li, X.; Liu, Z.; Lu, H.; Lu, Y.; Mao, Z.; Chen, X.; Li, N.; Ren, M.; et al. A Review on Predicting Ground $PM_{2.5}$ Concentration Using Satellite Aerosol Optical Depth. *Atmosphere* **2016**, *7*, 129. [CrossRef]
3. Zhang, W.; Xu, H.; Zheng, F. Aerosol Optical Depth Retrieval over East Asia Using Himawari-8/AHI Data. *Remote Sens.* **2018**, *10*, 137. [CrossRef]
4. Park, S.; Shin, M.; Im, J.; Song, C.K.; Choi, M.; Kim, J.; Lee, S.; Park, R.; Kim, J.; Lee, D.W.; et al. Estimation of ground-level particulate matter concentrations through the synergistic use of satellite observations and process-based models over South Korea. *Atmos. Chem. Phys.* **2019**, *19*, 1097–1113. [CrossRef]
5. Lee, A.; Jeong, S.; Joo, J.; Park, C.-R.; Kim, J.; Kim, S. Potential role of urban forest in removing $PM_{2.5}$: A case study in Seoul by deep learning with satellite data. *Urban Clim.* **2021**, *36*, 100795. [CrossRef]
6. Park, Y.; Kwon, B.; Heo, J.; Hu, X.; Liu, Y.; Moon, T. Estimating $PM_{2.5}$ concentration of the conterminous United States via interpretable convolutional neural networks. *Environ. Pollut.* **2020**, *256*, 113395. [CrossRef]
7. Park, S.; Lee, J.; Im, J.; Song, C.K.; Choi, M.; Kim, J.; Lee, S.; Park, R.; Kim, S.M.; Yoon, J.; et al. Estimation of spatially continuous daytime particulate matter concentrations under all sky conditions through the synergistic use of satellite-based AOD and numerical models. *Sci. Total Environ.* **2020**, *713*, 136516. [CrossRef]
8. Li, Y.; Chen, Q.; Zhao, H.; Wang, L.; Tao, R. Variations in PM_{10}, $PM_{2.5}$ and $PM_{1.0}$ in an Urban Area of the Sichuan Basin and Their Relation to Meteorological Factors. *Atmosphere* **2015**, *6*, 150–163. [CrossRef]
9. Guo, H.; Cheng, T.; Gu, X.; Wang, Y.; Chen, H.; Bao, F.; Shi, S.; Xu, B.; Wang, W.; Zuo, X.; et al. Assessment of $PM_{2.5}$ concentrations and exposure throughout China using ground observations. *Sci. Total Environ.* **2017**, *601*, 1024–1030. [CrossRef]

10. Ahn, C.; Torres, O.; Bhartia, P.K. Comparison of Ozone Monitoring Instrument UV Aerosol Products with Aqua/Moderate Resolution Imaging Spectroradiometer and Multiangle Imaging Spectroradiometer observations in 2006. *J. Geophys. Res. Atmos.* **2008**, *113*, D16. [CrossRef]
11. Choi, M.; Lim, H.; Kim, J.; Lee, S.; Eck, T.T.; Holben, B.B.; Garay, M.J.; Hyer, E.E.; Saide, P.P.; Liu, H. Validation, comparison, and integration of GOCI, AHI, MODIS, MISR, and VIIRS aerosol optical depth over East Asia during the 2016 KORUS-AQ campaign. *Atmos. Meas. Tech.* **2019**, *12*, 4619–4641. [CrossRef]
12. Levy, R.C.; Mattoo, S.; Munchak, L.A.; Remer, L.A.; Sayer, A.M.; Patadia, F.; Hsu, N.C. The Collection 6 MODIS aerosol products over land and ocean. *Atmos. Meas. Tech.* **2013**, *6*, 2989–3034. [CrossRef]
13. Gupta, P.; Remer, L.A.; Levy, R.C.; Mattoo, S. Validation of MODIS 3km land aerosol optical depth from NASA's EOS Terra and Aqua missions. *Atmos. Meas. Tech.* **2018**, *11*, 3145–3159. [CrossRef]
14. Crawford, J.H.; Ahn, J.-Y.; Al-Saadi, J.; Chang, L.; Emmons, L.K.; Kim, J.; Lee, G.; Park, J.-H.; Park, R.J.; Woo, J.H.; et al. The Korea–United States Air Quality (KORUS-AQ) field study. *Elem. Sci. Anthr.* **2021**, *9*, 00163. [CrossRef]
15. Giles, D.M.; Sinyuk, A.; Sorokin, M.G.; Schafer, J.S.; Smirnov, A.; Slutsker, I.; Eck, T.F.; Holben, B.N.; Lewis, J.R.; Campbell, J.R.; et al. Advancements in the Aerosol Robotic Network (AERONET) Version 3 database—Automated near-real-time quality control algorithm with improved cloud screening for Sun photometer aerosol optical depth (AOD) measurements. *Atmos. Meas. Tech.* **2019**, *9*, 169–209. [CrossRef]
16. Nakajima, T.; Tonna, G.; Rao, R.; Boi, P.; Kaufman, Y.; Holben, B. Use of sky brightness measurements from ground for remote sensing of particulate polydispersions. *Appl. Opt.* **1996**, *35*, 2672–2686. [CrossRef]
17. Hashimoto, M.; Nakajima, T.; Dubovik, O.; Campanelli, M.; Che, H.; Khatri, P.; Takamura, T.; Pandithurai, G. Development of a new data-processing method for SKYNET sky radiometer observations. *Atmos. Meas. Tech.* **2012**, *5*, 2723–2737. [CrossRef]
18. Alexandrov, M.D.; Lacis, A.A.; Carlson, B.E.; Cairns, B. Derivation of 2D fields of aerosol and trace gases parameters by integrated analysis of multi-instrument MFRSR dataset from DOE ARM program CART site. In *Remote Sensing of Clouds and the Atmosphere VI*; International Society for Optics and Photonics: Bellingham, WA, USA, 2002; Volume 4539, pp. 277–288.
19. Mok, J.; Krotkov, N.A.; Torres, O.; Jethva, H.; Li, Z.; Kim, J.; Koo, J.-H.; Go, S.; Irie, H.; Labow, G.; et al. Comparisons of spectral aerosol single scattering albedo in Seoul, South Korea. *Atmos. Meas. Tech.* **2018**, *11*, 2295–2311. [CrossRef]
20. Kerr, J.J.B. New methodology for deriving total ozone and other atmospheric variables from Brewer spectrophotometer direct sun spectra. *J. Geophys. Res. Atmos.* **2002**, *107*, D23. [CrossRef]
21. Che, H.; Shi, G.; Uchiyama, A.; Yamazaki, A.; Chen, H.; Goloub, P.; Zhang, X. Intercomparison between aerosol optical properties by a PREDE skyradiometer and CIMEL sunphotometer over Beijing, China. *Atmos. Chem. Phys.* **2008**, *8*, 3199–3214. [CrossRef]
22. Cheymol, A.; Sotelino, L.G.; Lam, K.S.; Kim, J.; Fioletov, V.; Siani, A.M.; Backer, H. De Intercomparison of aerosol optical depth from brewer ozone spectrophotometers and CIMEL sunphotometers measurements. *Atmos. Chem. Phys.* **2009**, *9*, 733–741. [CrossRef]
23. Di Sarra, A.; Sferlazzo, D.; Meloni, D.; Anello, F.; Bommarito, C.; Corradini, S.; De Silvestri, L.; Di Iorio, T.; Monteleone, F.; Pace, G.; et al. Empirical correction of multifilter rotating shadowband radiometer (MFRSR) aerosol optical depths for the aerosol forward scattering and development of a long-term integrated MFRSR-Cimel dataset at Lampedusa. *Appl. Opt.* **2015**, *54*, 2725–2737. [CrossRef]
24. Seo, S.; Kim, J.; Lee, H.; Jeong, U.; Kim, W.; Holben, B.N.; Kim, S.W.; Song, C.H.; Lim, J.H. Estimation of PM_{10} concentrations over Seoul using multiple empirical models with AERONET and MODIS data collected during the DRAGON-Asia campaign. *Atmos. Chem. Phys.* **2015**, *15*, 319–334. [CrossRef]
25. Lee, J.; Hong, J.W.; Lee, K.; Hong, J.; Velasco, E.; Lim, Y.J.; Lee, J.B.; Nam, K.; Park, J. Ceilometer Monitoring of Boundary-Layer Height and Its Application in Evaluating the Dilution Effect on Air Pollution. *Bound. Layer Meteorol.* **2019**, *172*, 435–455. [CrossRef]
26. Jung, J.; Kim, Y.J.; Lee, K.Y.; Cayetano, M.G.; Batmunkh, T.; Koo, J.-H.; Kim, J. Spectral optical properties of long-range transport Asian Dust and pollution aerosols over Northeast Asia in 2007 and 2008. *Atmos. Chem. Phys.* **2010**, *10*, 5391–5408. [CrossRef]
27. Kim, D.; Kim, J.; Jeong, J.; Choi, M. Estimation of health benefits from air quality improvement using the MODIS AOD dataset in Seoul, Korea. *Environ. Res.* **2019**, *173*, 452–461. [CrossRef]
28. Wang, J.; Li, Z. Estimation of ground-level dry $PM_{2.5}$ concentrations at 3 km resolution over Beijing using Geostationary Ocean Colour Imager. *Remote Sens. Lett.* **2020**, *11*, 913–922. [CrossRef]
29. Ahmad, M.; Alam, K.; Tariq, S.; Anwar, S.; Nasir, J.; Mansha, M. Estimating fine particulate concentration using a combined approach of linear regression and artificial neural network. *Atmos. Environ.* **2019**, *219*, 117050. [CrossRef]
30. Li, X.; Ma, Y.; Wang, Y.; Liu, N.; Hong, Y. Temporal and spatial analyses of particulate matter (PM_{10} and $PM_{2.5}$) and its relationship with meteorological parameters over an urban city in northeast China. *Atmos. Res.* **2017**, *198*, 185–193. [CrossRef]
31. Shin, U.; Park, S.H.; Park, J.S.; Koo, J.-H.; Yoo, C.; Kim, S.; Lee, J. bum Predictability of $PM_{2.5}$ in Seoul based on atmospheric blocking forecasts using the NCEP global forecast system. *Atmos. Environ.* **2021**, *246*, 118141. [CrossRef]
32. Rinnan, R.; Iversen, L.L.; Tang, J.; Vedel-Petersen, I.; Schollert, M.; Schurgers, G. Separating direct and indirect effects of rising temperatures on biogenic volatile emissions in the Arctic. *Proc. Natl. Acad. Sci. USA* **2020**, *117*, 32476–32483. [CrossRef] [PubMed]
33. Zhao, H.; Che, H.; Zhang, X.; Ma, Y.; Wang, Y.; Wang, H.; Wang, Y. Characteristics of visibility and particulate matter (PM) in an urban area of Northeast China. *Atmos. Pollut. Res.* **2013**, *4*, 427–434. [CrossRef]
34. Menares, C.; Gallardo, L.; Kanakidou, M.; Seguel, R.; Huneeus, N. Increasing trends (2001–2018) in photochemical activity and secondary aerosols in Santiago, Chile. *Tellus Ser. B Chem. Phys. Meteorol.* **2020**, *72*, 1–18. [CrossRef]

35. Koo, J.-H.; Kim, J.; Lee, Y.G.; Park, S.S.; Lee, S.; Chong, H.; Cho, Y.; Kim, J.; Choi, K.; Lee, T. The implication of the air quality pattern in South Korea after the COVID-19 outbreak. *Sci. Rep.* **2020**, *10*, 1–11. [CrossRef]
36. Shi, X.; Brasseur, G.P. The Response in Air Quality to the Reduction of Chinese Economic Activities during the COVID-19 Outbreak. *Geophys. Res. Lett.* **2020**, *47*, 11. [CrossRef]
37. Sorek-Hamer, M.; Franklin, M.; Chau, K.; Garay, M.; Kalashnikova, O. Spatiotemporal characteristics of the association between AOD and PM over the California Central Valley. *Remote Sens.* **2020**, *12*, 685. [CrossRef]
38. Zhai, S.; Jacob, D.J.; Brewer, J.F.; Li, K.; Moch, J.M.; Kim, J.; Lee, S.; Lim, H.; Lee, H.C.; Kuk, S.K.; et al. Interpretation of geostationary satellite aerosol optical depth (AOD) over East Asia in relation to fine particulate matter ($PM_{2.5}$): Insights from the KORUS-AQ aircraft campaign and seasonality. *Atmos. Chem. Phys. Discuss.* **2021**, 1–24. [CrossRef]
39. Eck, T.F.; Holben, B.N.; Kim, J.; Beyersdorf, A.J.; Choi, M.; Lee, S.; Koo, J.H.; Giles, D.M.; Schafer, J.S.; Sinyuk, A.; et al. Influence of cloud, fog, and high relative humidity during pollution transport events in South Korea: Aerosol properties and $PM_{2.5}$ variability. *Atmos. Environ.* **2020**, *232*, 117530. [CrossRef]
40. Koo, J.-H.; Lee, J.; Kim, J.; Eck, T.F.; Giles, D.M.; Holben, B.N.; Park, S.S.; Choi, M.; Kim, N.; Yoon, J.; et al. Investigation of the relationship between the fine mode fraction and Ångström exponent: Cases in Korea. *Atmos. Res.* **2021**, *248*, 105217. [CrossRef]
41. Zhang, M.; Ma, Y.; Shi, Y.; Gong, W.; Chen, S.; Jin, S.; Wang, J. Controlling factors analysis for the Himawari-8 aerosol optical depth accuracy from the standpoint of size distribution, solar zenith angles and scattering angles. *Atmos. Environ.* **2020**, *233*, 117501. [CrossRef]
42. Gao, L.; Chen, L.; Li, C.; Li, J.; Che, H.; Zhang, Y. Evaluation and possible uncertainty source analysis of JAXA Himawari-8 aerosol optical depth product over China. *Atmos. Res.* **2021**, *248*, 105248. [CrossRef]
43. Huang, G.; Chen, Y.; Li, Z.; Liu, Q.; Wang, Y.; He, Q.; Liu, T.; Liu, X.; Zhang, Y.; Gao, J.; et al. Validation and Accuracy Analysis of the Collection 6.1 MODIS Aerosol Optical Depth Over the Westernmost City in China Based on the Sun-Sky Radiometer Observations From SONET. *Earth Space Sci.* **2020**, *7*, 3. [CrossRef]
44. Yang, F.; Fan, M.; Tao, J. An improved method for retrieving aerosol optical depth using gaofen-1 wfv camera data. *Remote Sens.* **2021**, *13*, 280. [CrossRef]
45. Ghim, Y.S.; Chang, Y.S.; Jung, K. Temporal and spatial variations in fine and coarse particles in Seoul, Korea. *Aerosol Air Qual. Res.* **2015**, *15*, 842–852. [CrossRef]
46. Pan, L.; Xu, J.; Tie, X.; Mao, X.; Gao, W.; Chang, L. Long-term measurements of planetary boundary layer height and interactions with $PM_{2.5}$ in Shanghai, China. *Atmos. Pollut. Res.* **2019**, *10*, 989–996. [CrossRef]
47. Lee, J.; Koo, J.-H.; Kim, S.-M.; Lee, T.; Lee, Y.G. Comparison of aerosol properties in the Korean peninsula between AERONET version 2 and 3 dataset. *Asia Pac. J. Atmos. Sci.* **2021**, *57*, 629–643. [CrossRef]